Journal of Physiology (1992), **455**, *pp.* 339–365
With 7 figures
Printed in Great Britain

EQUILIBRIUM AND KINETIC STUDY OF GLYCINE ACTION ON THE *N*-METHYL-D-ASPARTATE RECEPTOR IN CULTURED MOUSE BRAIN NEURONS

BY JON W. JOHNSON* AND PHILIPPE ASCHER†

*From the *Department of Behavioral Neuroscience, University of Pittsburgh, Pittsburgh, PA 15260, USA and the †Laboratoire du Neurobiologie, Ecole Normale Supérieure, 46 rue d'Ulm, 75005 Paris, France*

(*Received 22 August 1991*)

SUMMARY

1. The characteristics of the activation of the *N*-methyl-D-aspartate (NMDA) response by glycine were studied using whole-cell and outside-out patch clamp recording techniques.

2. Glycine concentration–response (C–R) curves were measured in the presence of 10 μM-NMDA and fitted with the Hill equation modified to account for the response to NMDA observed in the absence of added glycine. The mean value of the apparent dissociation constant (K_D) was 150 nM, and the mean value of the Hill coefficient (n_H) was 1·1. When the K_D was corrected for the concentration of contaminating glycine in nominally glycine-free solutions, estimated assuming that there is no response in the absence of glycine, the value was 130 nM.

3. The question of how many glycine binding sites there are on each NMDA receptor–channel complex was addressed by examining the curvature at the foot of the glycine C–R curve. An equation that allowed estimation of both the concentration of contaminating glycine and of the value of n_H was fitted to glycine C–R data up to 50 nM. The mean value of n_H was found to be 1·0, consistent with the idea that there is one glycine binding site.

4. The kinetics of the interaction of glycine with the NMDA receptor were measured by fitting single exponential curves to the current relaxation following a jump in glycine concentration in the presence of 10 μM-NMDA. The plot of the inverse of the relaxation time constant as a function of glycine concentration after the concentration jump was linear. The association rate constant was estimated from these data as $1{\cdot}2 \times 10^7$ M^{-1} s^{-1} and the dissociation rate as 1·0 s^{-1}.

5. Experiments were devised to allow the evaluation of the K_D and dissociation rates of glycine in the absence of NMDA. They led to a value for K_D of 80 nM, slightly but significantly lower than the value of 150 nM estimated in the presence of 10 μM-NMDA. The glycine dissociation rate in the absence of NMDA was found to be 0·7 s^{-1}, not significantly different from that measured in the presence of 10 μM-NMDA.

6. The results are consistent with a model of the NMDA receptor with a single glycine binding site. The characteristics of glycine binding are similar in the absence

MS 9663

and the presence of 10 μM-NMDA, although NMDA binding may cause a small increase in the glycine K_D. Under the recording conditions used here, the dominant action of glycine on the NMDA response is not mediated through an effect on agonist binding at the NMDA site.

INTRODUCTION

Ligand-gated ion channels specifically activated by *N*-methyl-D-aspartate (NMDA receptors) are subject to regulation at an unusually large number of pharmacologically distinguishable sites (Collingridge & Lester, 1989). This paper concerns the mechanism by which the binding of glycine to the NMDA receptor interacts with the binding of NMDA to induce channel activation.

Much evidence has accumulated indicating that high affinity, strychnine-insensitive glycine binding sites in the brain (DeFeudis, Fando & Orensanz Muñoz, 1977; Kishimoto, Simon & Aprison, 1981; Bristow, Bowery & Woodruff, 1986) are responsible for the dependence of the NMDA response on glycine (Johnson & Ascher, 1987*a*). The interaction appears to be mediated by the binding of glycine directly to the NMDA receptor without need for intracellular messengers or energy sources, since glycine action is rapid and its effects can be observed with outside-out patches. Glycine binding is probably required for channel opening to occur (Kleckner & Dingledine, 1988).

The presence of a glycine site on NMDA receptors has been widely documented (see Thomson, 1990). Equilibrium binding as well as electrophysiological studies have confirmed the high affinity of glycine for its site, with reported values of the apparent dissociation constant varying from less than 100 nM to 700 nM, and values for the Hill coefficient varying from 0·9 to 1·5 (DeFeudis *et al.* 1977; Kishimoto *et al.* 1981; Bristow *et al.* 1986; Johnson & Ascher, 1987*b*; Reynolds, Murphy & Miller, 1987; Fong, Davidson & Lester, 1988; Kleckner & Dingledine, 1988; Kushner, Lerma, Zukin & Bennett, 1988; Snell, Morter & Johnson, 1988; Bonhaus, Yeh, Skaryak & McNamara, 1989; Huettner, 1989; Kessler, Terramani, Lynch & Baudry, 1989; Vyklický, Benveniste & Mayer, 1990). The kinetic properties of the interaction of glycine with its receptor have been investigated by analysis of the current relaxations following glycine concentration jumps (Ascher & Johnson, 1989; Benveniste, Clements, Vyklický & Mayer, 1990*a*; Benveniste, Mienville, Sernagor & Mayer, 1990*b*; Benveniste & Mayer, 1991).

We describe here three groups of experiments used to evaluate the number and apparent affinity of glycine binding sites. In equilibrium experiments, we have measured the apparent dissociation constant of the potentiation produced by glycine and examined the curvature of the glycine concentration–response curve at low glycine concentrations. In kinetic experiments we have performed glycine concentration jumps and attempted to deduce from the analysis of the resulting current relaxations the rates of association and dissociation of glycine. In the final group of experiments we devised a protocol to evaluate the characteristics of glycine action in the absence of NMDA.

Benveniste *et al.* (1990*a*, *b*) and Benveniste & Mayer (1991) have proposed a model in which each NMDA receptor–channel complex bears two identical binding sites for glycine, and in which the occupation of both sites is necessary for channel opening.

The results we have obtained favour a model in which glycine action is mediated by the binding of glycine to a single site on each NMDA receptor–channel complex. The reasons for our differing results are not clear. They may be related, however, to another major difference between their results and ours. Under our experimental conditions, we have observed marked desensitization following a jump into 100 μM-NMDA at any glycine concentration (Sather, Johnson, Henderson & Ascher, 1990; Sather, Dieudonné, MacDonald & Ascher, 1992), while they have described a form of desensitization that is prevented at high glycine concentrations (Vyklický *et al.* 1990; Benveniste & Mayer, 1991). We wanted to minimize the possible contamination of current relaxation measurements by glycine-insensitive desensitization. We therefore performed experiments at an NMDA concentration of 10 μM, or else deduced the characteristics of glycine binding in the absence of NMDA.

A preliminary version of this work has been previously reported (Johnson & Ascher, 1987*b*).

METHODS

Whole-cell and outside-out patch recordings (Hamill, Marty, Neher, Sakmann & Sigworth, 1981) were made from cortical and diencephalic neurons from 15- to 16-day-old mouse embryos in primary culture as previously described (Ascher, Bregestovski & Nowak, 1988). Recording pipettes with resistances of 3 to 7 MΩ were used. In most cases the pipettes were coated with Sylgard (Rhône-Poulenc, Paris, France) and fire polished. The intracellular (pipette) solution was composed of (mM): CsF, 120; CsCl, 20; EGTA-Cs, 10; HEPES, 10. The pH was adjusted to 7·2 with CsOH. The extracellular solution contained (mM): NaCl, 140; KCl, 2·8; $CaCl_2$, 1; HEPES, 10. In addition, 0·2 μM-TTX was added during experiments. pH was adjusted to 7·2 with NaOH. All experiments were performed at room temperature (16–26 °C).

In all experiments a holding potential of −50 mV was used. Membrane current was measured with a List EPC-7 patch-clamp amplifier. Data were recorded on a Racal FM tape recorder and a Gould Brush 280 chart recorder. In order to analyse current relaxations, current records were replayed from the tape recorder, filtered (Frequency Devices Series 900 8-pole Butterworth filter; corner frequency as indicated in figure legends), and digitized with an Axolab 1 system (Axon Instruments). The records were averaged and when necessary fitted with single exponentials using Axess software (Axon Instruments). Curve fitting of concentration–response data such as in Figs 1, 2 and 6, and single exponential fits such as in Fig. 7, were performed on a Minc PDP 11/23 using the equations described in the text and a curve fitting program based on the simplex algorithm (Caceci & Cacheris, 1984). Best fit was defined as the set of parameter values that minimized the sum of the squared differences between data points and fit line. In concentration–response curves, inward currents are expressed as absolute values. Means are expressed ± standard deviation.

During experiments, the extracellular solution bathing the cell or patch under study was controlled with a multi-barrel fast perfusion system (Johnson & Ascher, 1987*a*; Sather *et al.* 1990). Two or three parallel glass capillary tubes with inner diameters of about 500 μm were glued together side by side and held by a rod attached to a Leitz micromanipulator. Each barrel was connected by capillary tubing to a reservoir of perfusion fluid. The rate of flow of fluid out of the barrels was controlled by a peristaltic pump. During concentration jumps, the solutions were forced out of the barrels at a rate of about 0·4 ml min^{-1}, which corresponds to a velocity of 3·4 cm s^{-1} at the barrel orifice. The assembly was manipulated so that one barrel was within 100 μm of and facing the cell or patch under study. The exterior of the cell or patch was thus exposed only to the solution flowing out of that barrel. In order to change solutions, the barrel assembly was moved laterally by the Leitz manipulator a distance of one barrel diameter. The adjacent barrel was then centred over the cell or patch, which was thus exposed exclusively to the solution flowing out of the new barrel. In order to allow rapid and well controlled barrel movements, a stepper motor was used to turn the appropriate axis of the micromanipulator. Under stepper motor control, barrel movement took about 50 ms. The timing and amount of stepper motor rotation was determined by a stepper motor controller that received movement commands from a computer.

Thus, a rapid sequence of solution changes, or a large number of repetitive solution changes, could easily be performed under computer control. The computer produced a trigger signal during each barrel movement that allowed precise determination of the time of barrel movement and averaging of responses to repeated concentration jumps.

NMDA was obtained from Cambridge Research Biochemicals, Cambridge, UK and glycine from Prolabo, Paris, France.

RESULTS

Glycine concentration–response curves at equilibrium

The glycine concentration dependence of the whole-cell response to 10 μM-NMDA was studied using glycine concentration–response (C–R) curves. The steady state current was measured as a function of the concentration of added glycine. A modified form of the Hill equation was fitted as described in Methods to data collected from a single cell. The equation used was:

$$R_G = R_0 + (R_M - R_0)\{[G]^{n_H}/([G]^{n_H} + K_D{}^{n_H})\}, \quad (1)$$

where R_G is the net membrane current activated by perfusion of 10 μM-NMDA plus an added glycine concentration [G], R_0 is the response to 10 μM-NMDA in the absence of added glycine, R_M is the maximal response at a saturating glycine concentration, K_D (the apparent dissociation constant of glycine) is the glycine concentration at which $(R_M - R_0)$ is half its maximal value, and n_H is the Hill coefficient for glycine. In these experiments [G] is the only independent variable, R_0 and each value of R_G were measured response magnitudes, and the values of the free parameters R_M, K_D and n_H were determined by the fitting procedure. C–R data from a cell were accepted only if responses at five or more different glycine concentrations were measured. Because the reliability of curve fitting was increased when the data clearly established a plateau near the maximal response, C–R data were also required to include at least two points at glycine concentrations at or above 1 μM.

In Fig. 1*B*, an example of a C–R curve is shown. From fits to a total of fourteen C–R curves, each in a different cell, we calculated a mean K_D of 150 ± 60 nM, and a mean value of n_H of $1{\cdot}11 \pm 0{\cdot}19$. This value of n_H is just significantly greater than 1 ($0{\cdot}02 < P < 0{\cdot}05$, 1-tailed Wilcoxon signed-ranks test). The mean value of the squared correlation coefficient (r^2) for the fourteen fits was 0·995.

In nearly all experiments there was a measurable response to 10 μM-NMDA in the absence of added glycine. This response was probably due at least in part to the presence of contaminating glycine. The entire response in the absence of added glycine must have depended on the presence of contaminating glycine if, as first suggested by Kleckner & Dingledine (1988), there is no NMDA response in the complete absence of glycine. If this is the case, then in general eqn (1) should not accurately describe the C–R data. The values of K_D and n_H estimated by fitting eqn (1) to the data would differ from the true values that describe the relation between response magnitude and actual glycine concentration.

In the special case where n_H is equal to 1, however, eqn (1) can be expected to accurately fit the C–R data. The presence of contaminating glycine would only alter the estimated value of K_D (shifting the C–R curve to the right) without having an effect on n_H (see Appendix 1). Assuming, as we will suggest below, that n_H is equal to 1, we corrected the value of each K_D estimated from fitting eqn (1) to a C–R curve

for the error due to contaminating glycine. The mean corrected value of K_D was found to be 130 ± 60 nM ($n = 14$).

The equations of Appendix 1 also allow estimation of the concentration of contaminating glycine in each experiment. In early experiments (such as that

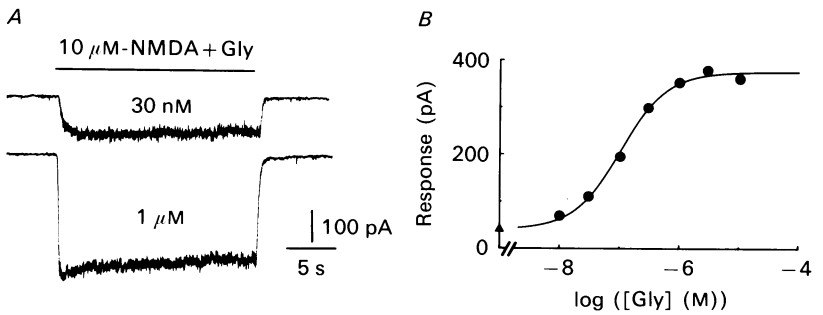

Fig. 1. Measurement and fitting of glycine concentration–response (C–R) curves. *A*, examples of data used for C–R curves. Responses to the application of 10 μM-NMDA plus the indicated concentration of glycine are shown. The data are from a whole-cell recording. Holding potential was −50 mV. Data were filtered at an effective frequency of 100 Hz by the chart recorder used to make this figure. *B*, C–R data from the same cell are plotted. Whole-cell current was measured (relative to current in the absence of NMDA) at least 5 s after application of NMDA after having reached a steady level. Whole-cell current in the presence of the indicated concentration of glycine (●) and whole-cell current in the absence of added glycine (R_0; 40 pA; ▲) are plotted. The data were fitted (continuous line) as described in Methods by eqn (1). The results of the fit are: maximum response (R_M), 330 pA; apparent affinity (K_D), 100 nM; Hill coefficient (n_H), 1·15; squared correlation coefficient (r^2), 0·994. C–R curves from fourteen different cells were measured and fitted. Five to sixteen points were included in each C–R curves. If any measured currents were greater than 1 nA, the experiment was not included. If any measured currents were between 0·5 and 1 nA, current values were corrected for a series resistance of 5 to 14 MΩ, assuming a linear *I–V* relationship and reversal potential of 0 mV.

illustrated in Fig. 1), in order to minimize glycine contamination, solutions were made up fresh each day from frozen stock solutions, and drug-containing stock solutions were diluted at least 100-fold into the perfusion solution immediately before application to the cell under study. Double glass-distilled water was used for all solutions. For experiments in which no further precautions were taken, the mean concentration of contaminating glycine was calculated to be 22 ± 20 nM ($n = 11$). In some later experiments, all glassware was in addition soaked in distilled water for several hours before use. In these experiments, the mean calculated concentration of contaminating glycine was $2{\cdot}7 \pm 1{\cdot}6$ nM ($n = 3$). The calculated concentration of contaminating glycine was significantly decreased by soaking the glassware ($P < 0{\cdot}01$; one-tailed Mann–Whitney test), indicating that the glassware was a significant source of glycine contamination. The small magnitude of the response in the absence of added glycine, and the low level of the glycine contamination calculated assuming that glycine binding is necessary for NMDA receptor activation, support the idea (Kleckner & Dingledine, 1988) that there is very little or no NMDA response in the true absence of glycine.

The value of n_H estimated from C–R curves (1·11) suggests that the response to glycine exhibits little co-operativity. However, fitting of entire concentration–response curves provides a relatively insensitive measure of co-operativity. In addition, the presence of a 'slow' desensitization process ($\tau > 1$ s) that is thought to depend at least in part on Ca^{2+} influx (Mayer & Westbrook, 1985; Mayer, MacDermott, Westbrook, Smith & Barker, 1987; Clark, Clifford & Zorumski, 1990; Vyklický *et al.* 1990) and thus on current magnitude could bias estimates of n_H based on entire C–R curves. A further problem with the use of eqn (1) to estimate the degree of co-operativity is that the data should only be well fitted if n_H is equal to 1.

These limitations can be minimized or eliminated by estimating the degree of co-operativity from the curvature at the foot of the C–R curves. This method for estimating n_H is superior to the fitting of the entire C–R curve for several reasons: (1) the estimated value of n_H will be a more sensitive measure of co-operativity, and should correspond better with the number of binding sites under a far wider variety of binding schemes; (2) interference from any desensitization-like process that depends on current magnitude should be minimized by using only the smaller responses measured at low glycine concentrations; and (3) the measurement of co-operativity can be made despite the presence of an unknown background glycine contamination (see below).

The measurement of n_H from the foot of C–R curves is typically made from a log–log plot. However, such a plot cannot be validly used here because of the unknown background glycine contamination. Instead, the following equation was fitted to the untransformed data:

$$R_G = M([G]_A + [G]_B)^{n_H}, \quad (2)$$

where R_G is the net membrane current activated by perfusion of 10 μM-NMDA plus an added glycine concentration of $[G]_A$, $[G]_B$ is the background glycine contamination, n_H is the Hill coefficient, and M is a parameter that depends on response magnitude. In these experiments $[G]_A$ is the only independent variable and R_G is the only dependent variable. The equation was fitted to the data as described in Methods to determine the values of the free parameters M, $[G]_B$, and n_H that gave the best fit. The parameter n_H corresponds to the Hill coefficient determined traditionally from the slope of a log–log plot. Because the background glycine contamination is estimated and accounted for, its presence should not interfere with the estimate of n_H (point (3), above).

Only data up to a maximum added glycine concentration of 50 nM, about 1/3 of the previously estimated K_D, was used. This maximum concentration was chosen because the inclusion of points at higher concentrations tended to decrease the estimated n_H, but deletion of points at 50 nM or lower had no consistent effect on the estimated n_H. Because a small amount of 'fast' desensitization ($\tau < 200$ ms; see Benveniste *et al.* 1990*a*; Sather *et al.* 1990, 1992; Shirasaki, Nakagawa, Wakamori, Tateishi, Fukuda, Murase & Akaike, 1990) was observed even at an NMDA concentration of 10 μM, measurements of both the peak and steady state responses were made. An example of the results of one such experiment is shown in Fig. 2. From three such experiments, the mean value of n_H, estimated using eqn (2), was: peak response, $1{\cdot}03 \pm 0{\cdot}18$; steady state response, $0{\cdot}96 \pm 0{\cdot}15$. The mean value of $[G]_B$, the

background glycine contamination estimated from eqn (2) was (nM): peak response, 6·5±6·6; steady state response, 4·8±3·8. The mean value of r^2 for the fit of eqn (2) to the data was: peak response, 0·996; steady state response, 0·994. In all three experiments, the glassware was soaked as previously described to reduce background

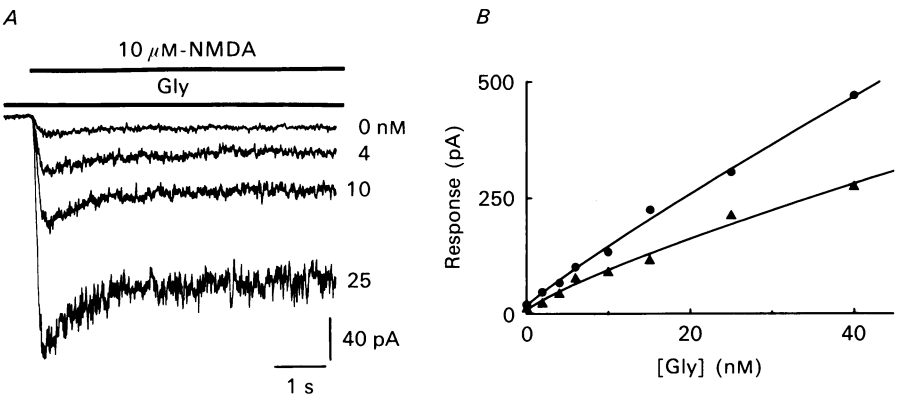

Fig. 2. Estimation of co-operativity of glycine binding from the foot of the C–R curve. *A*, examples of data used to plot the foot of the C–R curve. Responses to the application of 10 μM-NMDA plus the indicated concentration of glycine are superimposed. Data from a single whole-cell recording. Each trace is the average of two to six records. Data were filtered at 80 Hz and sampled at 200 Hz. *B*, C–R data from the same cell. Whole-cell current at its peak (●) and at steady-state (▲) are plotted as a function of added glycine concentration. The data were fitted (continuous line) as described in Methods by eqn (2). The values of n_H estimated from the fits are: peak response, 0·89; steady state response, 0·85. The background glycine concentrations ($[G]_B$) estimated from the fits are (mM): peak response, 1·0; steady state response, 0·8. The values of r^2 for the fits are: peak response, 0·995; steady state response, 0·998. The foot of the C–R curve from two other cells was similarly measured and fitted. The maximum glycine concentration used for the fits was 50 nM. Six to ten points were included in each fit.

glycine contamination. These data suggest that the response to glycine does not exhibit positive co-operativity.

Kinetics of glycine binding

When the solution perfusing a cell is quickly changed from control solution to one containing NMDA plus glycine at a concentration well below the glycine apparent dissociation constant, the response magnitude reached its steady state level slowly (see, e.g., the current response in Fig. 1*A* at 30 nM-glycine). This slow increase probably does not reflect the speed of solution change: jumps into higher concentrations of glycine (see, e.g., the current response in Fig. 1*A* at 1 μM-glycine) or into NMDA (see Fig. 3*A*) resulted in much faster current relaxations. One possible explanation for the slow response is that the binding kinetics of low concentrations of glycine with its receptor limit the rate at which the NMDA response increases. If this is so, it should be possible to measure the rate constants of glycine association and dissociation from current relaxations following glycine concentration jumps.

In the experiment of Fig. 1, both the glycine and NMDA concentrations were

changed simultaneously. The response kinetics can be expected to be complex in this situation, as they appear to be. In the experiments described in Figs 3*B* to 5, 10 μM-NMDA was included in the solutions flowing out of both barrels 1 and 2 of the multiple-barrel fast perfusion system, and glycine was added to only one of the two solutions. Thus jumps into and out of various glycine concentrations were made in the presence of a constant NMDA concentration.

In order to interpret the results of such experiments, it is instructive to examine the predictions of the simplest plausible model of the interaction of glycine with its receptor site. If there is only one glycine binding site on the NMDA receptor (as suggested by the C–R data), then the model can be written:

$$R + G \underset{k_-}{\overset{k_+}{\rightleftharpoons}} RG, \tag{3}$$

where G is a glycine molecule, R is the NMDA receptor with no glycine bound, RG is the NMDA receptor with glycine bound, k_+ is the glycine association rate constant, and k_- is the glycine dissociation rate constant. The apparent dissociation constant is

$$K_D = k_-/k_+. \tag{4}$$

The relaxation following a jump in glycine concentration should follow a time course described by

$$I(t) = I_f + (I_i - I_f)\exp(-t/\tau), \tag{5}$$

where $I(t)$ is the measured whole-cell current at time t, I_i is the current just before the jump in glycine concentration, I_f is the steady state response following the glycine concentration jump, and τ is the time constant of the current relaxation following the jump. In this model, the value of τ can be calculated from the equation

$$\tau = 1/(k_+[G] + k_-), \tag{6}$$

where [G] is the glycine concentration following the jump.

This model is clearly an oversimplification. The current measured following a jump in glycine concentration depends on the interaction of NMDA with its receptor site(s) and channel opening and closing, as well as on glycine binding. Equation (3) ignores these other processes. However, if the kinetics of NMDA binding and of channel transitions are much faster than the time constant of the relaxation in glycine binding, then the current relaxation will approximate the relaxation of glycine binding (see Appendix 2).

It is important to establish approximately how slow current relaxations must be in order for them to exhibit little dependence on channel transition or NMDA binding kinetics. The arithmetic mean open time of NMDA channels has been measured in the 4–10 ms range (Nowak, Bregestovski, Ascher, Herbet & Prochiantz, 1984; Ascher *et al.* 1988; Howe, Colquhoun & Cull-Candy, 1988), suggesting relaxation kinetics must be much faster than those that will be examined here. However, this conclusion may not be valid because the mean open time histogram generally cannot be characterized by a single open time (Howe, Cull-Candy & Colquhoun, 1991), and very long openings are sometimes observed (Jahr & Stevens,

1987). A safer manner for establishing a limit on how slow channel kinetics could be is to look at macroscopic NMDA current relaxations. Relaxation time constants of less than 30 ms have been measured following concentration jumps between 0 and 100 μM-NMDA, jumps into high glycine concentrations, and jumps in the concentration of low affinity glycine agonists (Benveniste *et al.* 1990*b*; J. W. Johnson & P. Ascher, unpublished observations). Because these relaxations cannot be faster than the limits imposed by channel kinetics, they indicate that channel and NMDA binding kinetics must be much faster than the relaxations examined here.

A further concern is whether or not the speed of solution change is fast enough to allow measurement of current relaxations limited by glycine binding kinetics. As long as current measurements are not begun until after the solution change is complete, the remaining decay should not be influenced by the speed of the preceding solution change. However, if the change is slow relative to binding kinetics, the decay due to glycine binding cannot be practically measured in isolation.

In order to establish the fastest relaxation that could be used to determine glycine binding kinetics under our experimental conditions, jumps were made between 0 and 10 μM-NMDA while holding glycine concentration constant at 10 μM. The resulting current decay must depend on the combined effects of the kinetics of NMDA binding, of channel transitions, and of solution changes (which may be slowed by diffusion in the extracellular space), and cannot be faster than the slowest of them. Time constants were estimated from single exponential fits made to averages of two to four current relaxations following NMDA concentration jumps in each cell. From five experiments, the mean decay time constant for the current decay following jumps into 10 μM-NMDA was 54 ± 11 ms, and for jumps from 10 μM-NMDA to 0 NMDA it was 77 ± 5 ms (Fig. 3*A*).

The relaxation following a jump of NMDA concentration as measured here probably does not provide an accurate estimate of either the speed of the solution change or the time constants that characterize NMDA binding kinetics. It is likely that the speed of both processes is underestimated because both (and possibly also channel kinetics) contribute to the relaxation. However, this measurement is particularly useful as a conservative estimate of how quickly a concentration change can be made at NMDA receptors. First, a concentration of NMDA below its dissociation constant was used, so the current relaxation could not be complete before the concentration change was complete. Second, the relaxation depends on the concentration change at regions where NMDA receptors are located. Because some receptors may be on cell processes apposed to glial cell membrane, approaches for estimating speed of solution change that do not depend on a concentration change of a molecule that binds to the NMDA receptor might provide an overestimate. In some experiments, particularly on neurons from older (2 or 6 weeks) cultures, much slower current relaxations were observed. Such cells were not used for relaxation experiments. The possibility remains that these measurements provide an overestimate of the speed of glycine concentration changes because diffusion of glycine may be more strongly buffered than diffusion of NMDA. This possible source of error will be addressed below with relaxation measurements from outside-out patches.

If measurements can be made under conditions in which the current decay reflects glycine binding kinetics, and the single site model is correct, then several predictions

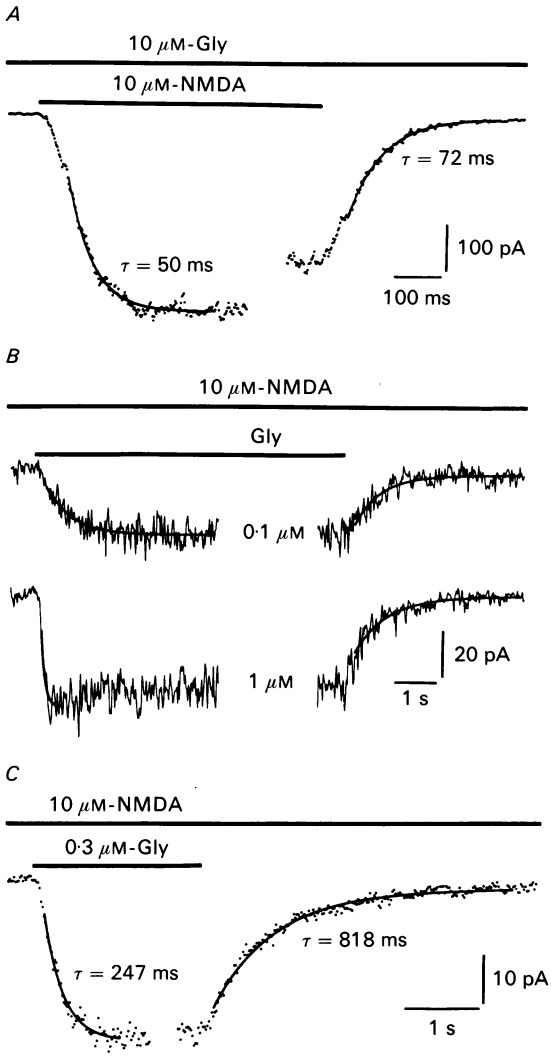

Fig. 3. Whole-cell recordings of current relaxations following concentration jumps. *A*, the concentration of NMDA was jumped from 0 to 10 μM (left) and then from 10 μM to 0 (right) while maintaining a constant glycine concentration of 10 μM. Both traces are the average of four current relaxations in the same cell. Data were filtered at 200 Hz and sampled at 500 Hz, and a single exponential was fitted between 80 and 380 ms after fast perfusion barrel movement. Averaged data are shown as dots, fit as a continuous line. The time constants estimated from the fits are shown. Similar measurements were made from four other cells. *B*, unaveraged responses to concentration jumps between 0 added glycine and the indicated concentration in a constant NMDA concentration of 10 μM. Single exponential fits are shown as continuous lines. Single exponential fits to unaveraged data were not used for further analysis. *C*, jumps were made between 0 and 0·3 μM added glycine in the constant presence of 10 μM-NMDA. Each trace is the average of twelve jumps. Single exponential fits (continuous lines) were made between 0·2 and 1·2 s (left) and between 0·2 and 4·2 s (right) after fast perfusion barrel movement. Time constants of single exponential fits are shown. Data were filtered at 20 Hz and sampled at 50 Hz. Nine relaxation time constants following jumps into glycine and twenty relaxation time constants following jumps into 0 added glycine were measured similarly in twelve different whole-cell experiments. Fits of whole-cell data were always begun 0·2 s after fast perfusion barrel movement to ensure that the solution change was complete.

about the data can be made: (1) the relaxations should follow a single exponential time course (see eqn (5)); (2) the time constant of the relaxation should not depend on the glycine concentration before the jump; (3) the time constant of the relaxation should depend on the glycine concentration after the jump as described by eqn (6); and (4) the value of K_D for glycine derived from eqn (4) using the values of k_+ and k_- derived from relaxation measurements should approximate the K_D value measured from C–R curves.

Unaveraged data from jumps between 0 added glycine and 0·1 or 1·0 μM-glycine are shown in Fig. 3*B*. As predicted by eqns (5) and (6), the relaxations appear to take place more quickly following jumps into higher glycine concentrations, and to be slowest following jumps into 0 added glycine. The single exponential nature of the relaxations can be better judged from averages of the current decay following concentrations jumps (Fig. 3*C*). The decays were consistently well fitted by a single exponential, as predicted by eqn (5).

The data shown in Fig. 3*A* suggests that the speed of solution changes could not cause the slow relaxations observed following glycine concentration jumps. However, it is conceivable that repetitive binding of glycine to a population of glycine binding sites in a region of restricted diffusion could act specifically to slow both the rise and the decay time of the glycine concentration. Regions of restricted diffusion might exist, for example, due to the close apposition of dendritic and glial cell membrane. In order to assure that the recorded relaxations were not artifactually slowed by any process involving regions of restricted diffusion, the relaxation measurements were repeated on isolated outside-out patches. Because such patches are held well above the cells on the bottom of the dish, and the perfusion stream is directed onto the patch, there should be no regions of restricted diffusion. As can be seen in Fig. 4*A*, relaxation time constants could not be estimated from single jumps in glycine concentration because of the relative infrequency of channel transitions. However, following the averaging of current records of 21 to 170 glycine concentration jumps, it was possible to fit a single exponential to the relaxations. The time constants measured in outside-out experiments were consistent with those measured in whole-cell experiments following the same jump in glycine concentration (see Fig. 5).

In order to evaluate the consistency of these relaxation measurements with the hypothesis that they reflect the kinetics of glycine binding, and to derive information about binding rate constants, the relation between the relaxation time constant and glycine concentration was studied. Both the time constant of the current decay following a concentration jump into 0 added glycine (τ_{off}) and the time constant of the current decay following a concentration jump from 0 added glycine into a higher glycine concentration (τ_{on}) were measured as a function of glycine concentration. In Fig. 5*A*, $1/\tau_{off}$ is plotted as a function of the glycine concentration before the jump. If there were any dependence of τ_{off} on the glycine concentration before a jump, it would suggest that the perfusion system does not make complete and rapid solution changes. As shown in Fig. 5*A*, τ_{off} remained independent of glycine concentration before the jump over a 100-fold concentration range.

In Fig. 5*B*, both $1/\tau_{off}$ and $1/\tau_{on}$ are plotted as a function of the glycine concentration following the concentration jump. Equation (6) predicts a straight line relation, with the slope equal to k_+ and the y-intercept equal to k_-. The plotted values appear consistent with a linear relationship, with $k_+ = 1{\cdot}2 \times 10^7$ M s^{-1} and $k_- = 1{\cdot}0$ s^{-1}.

Although the y-intercept of the linear fit to both $1/\tau_{off}$ and $1/\tau_{on}$ plotted in Fig. 5B should provide the best estimates of k_+ and k_-, k_- can be estimated in two independent ways. First, the average of all values of $1/\tau_{off}$ can be used. These data provide a value of $1{\cdot}0 \pm 0{\cdot}4\ s^{-1}$ ($n = 27$) for k_-. Second, the linear fit shown in

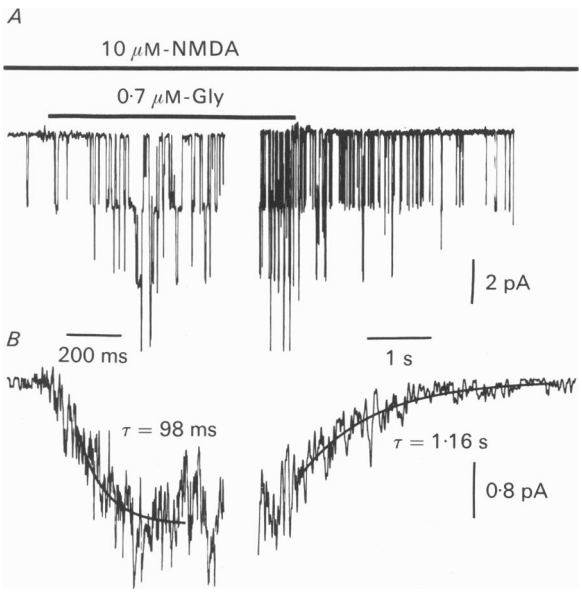

Fig. 4. Current relaxations following glycine concentration jumps measured from an outside-out patch. A, single (unaveraged) record of patch current following jumps between 0 added glycine and 0·7 μM added glycine. The NMDA concentration was maintained at 10 μM throughout the experiment. Data were filtered at 0·5 kHz and sampled at 1 kHz. B, averaged relaxations from the same cell. Average of twenty-five jumps (left) or twenty-three jumps (right). Before averaging data were filtered at 0·5 kHz and sampled at 1 kHz (left) or filtered at 20 Hz and sampled at 200 Hz (right). Smooth lines are single exponential fits to the averaged data. Fits were made to data between 0·1 to 0·5 s after barrel movement (left) or 0·1 to 4·1 s after barrel movement (right). Time constants of fits are shown in the figure. Note in both A and B that the time scale used on the left is not the same as that used on the right. Six relaxation time constants following jumps into glycine and seven relaxation time constants following jumps into 0 added glycine were similarly measured in four different outside-out patch experiments. Fits of patch data were always begun 0·1 s after fast perfusion barrel movement to ensure that the solution change was complete.

Fig. 5B can be made only to the twelve values of $1/\tau_{on}$ and the line extrapolated to the y-intercept. This approach provides a value of $0{\cdot}8\ s^{-1}$. The similarity of these two values is consistent with the simple model of glycine binding described above.

The final prediction that was made from the hypothesis that these relaxations are a reflection of glycine binding kinetics was that the ratio k_-/k_+ derived from relaxation measurements should approximate the K_D measured from C–R curves.

k_-/k_+ is 90 nM, in reasonable agreement with the value of 150 ± 60 nM for the K_D estimated independently from C–R curves. These data support the idea that the relaxation measurements do indeed reflect the kinetics of interaction of glycine with its receptor site on the NMDA receptor.

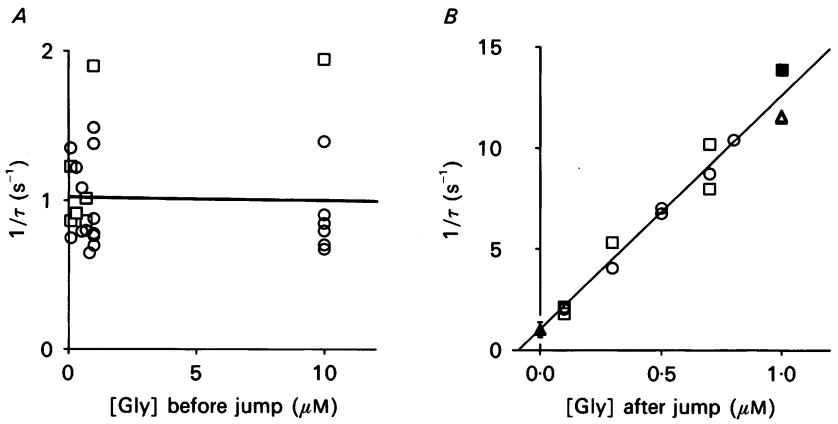

Fig. 5. Plots of $1/\tau$ as a function of glycine concentration. *A*, relaxations following jumps into 0 added glycine. On the abscissa is plotted the glycine concentration before the concentration jump. In each case a concentration jump was made from the indicated glycine concentration (0·1, 0·3, 0·5, 0·7, 0·8, 1·0 or 10·0 μM) to a solution with no added glycine. Time constants were measured as shown in Figs 3 and 4. Each point is from a separate whole-cell (○) or outside-out patch (□) experiment. The line is a least-squares fit to the data. The slope of the line is $-2{\cdot}53 \times 10^3$ M^{-1} s^{-1}, which is not significantly different from 0 ($P > 0{\cdot}5$). The value of r^2 for the fit is $9{\cdot}4 \times 10^{-4}$. *B*, relaxations following all glycine concentration jumps. On the abscissa is plotted the glycine concentration following the concentration jump. Each point is from a single measurement made either with a whole-cell (○ and △) or an outside-out patch (□ and ■) recording, except the point at 0 added glycine (▲), which shows the mean value of $1/\tau_{off}$ (standard deviation indicated on plot; $n = 27$). These are the same twenty-seven values of $1/\tau$ that are plotted in Fig. 5*A* against the glycine concentration before the concentration jump. The continuous line is a least-squares fit to a total of thirty-nine points: twenty-seven points at 0 glycine (summarized by ▲), and twelve points (○ and □) at other glycine concentrations. Relaxations measured following jumps into 1 μM-glycine (whole-cell, △; outside-out patch, ■) were not used to calculate the least-squares fit because the time constants were considered too close to the fastest relaxation that could be reliably measured. However, the points are plotted to show that they are not inconsistent with the other data. The slope of the fit line is $1{\cdot}16 \times 10^7$ M^{-1} s^{-1}. The value of r^2 for the line is 0·977. In all experiments, the NMDA concentration was maintained at 10 μM throughout the concentration jumps.

The data presented thus far were obtained in the presence of 10 μM-NMDA. We were interested in observing the interaction of glycine with the NMDA receptor over a range of NMDA concentrations. If glycine modifies the affinity of NMDA, the converse should be true and the apparent glycine affinity would be different when measured at NMDA concentrations higher or lower than 10 μM. Interpretation of the data measured at higher NMDA concentrations would be complicated, however, at

least in part because the various processes of desensitization (Mayer & Westbrook, 1985; Mayer *et al.* 1987; Benveniste *et al.* 1990*a*; Clark *et al.* 1990; Sather *et al.* 1990, 1992; Shirasaki *et al.* 1990; Vyklický *et al.* 1990), which are imperfectly understood, would be exaggerated. Desensitization is in some cases already visible at 10 μM-NMDA (see, e.g., Fig. 2*A*).

Despite these difficulties, several attempts were made to measure the kinetics of glycine binding at NMDA concentrations of 50 to 500 μM. The current relaxations following glycine concentration jumps were often found to be better fitted by double than single exponentials, which we provisionally attributed to the complications arising from desensitization. However, the main component of τ_{off} had a slow time constant (close to 1 s) similar to that found at 10 μM-NMDA.

Glycine binding in the absence of NMDA

Because of their complexity, we did not further analyse data collected in the presence of NMDA concentrations higher than 10 μM. However, the measurement of glycine binding in the absence of NMDA, if feasible, would provide the advantage of allowing investigation of NMDA-dependent changes in glycine binding while minimizing the complications resulting from desensitization. Comparison of glycine binding characteristics at 0 and 10 μM-NMDA would not reveal interactions between NMDA and glycine binding as sensitively as a comparison made at NMDA concentrations well below and above the K_D for NMDA. However, if NMDA binding has a large effect on glycine binding, then measurements made in the absence of NMDA should differ from those described above. An extreme case, such as a requirement that NMDA be bound before glycine could bind, would be obvious.

In order to study the apparent dissociation constant of glycine from NMDA receptors in the absence of NMDA, a 3 barrel fast perfusion system was used. In barrel 1 was the concentration of glycine to be tested, in barrel 2 was control solution with no drugs added, and in barrel 3 was 10 μM-NMDA with no added glycine The cell was first perfused with the solution flowing out of barrel 1 for at least 10 s to allow equilibrium binding of the glycine in the barrel to the NMDA receptor. The barrels were then moved so that the cell was exposed to the solution in barrel 2 for 0·5 s to completely wash away unbound glycine. The barrels were then moved again so that the cell was exposed to the solution in barrel 3, and the response to NMDA recorded. In the extreme case that no glycine binding to the NMDA receptor could occur in the absence of NMDA, the response to barrel 3 should not be influenced by the previous exposure to glycine, but rather should depend only on the concentration of contaminating glycine and of NMDA in the barrel 3 solution. However, if glycine did bind during the exposure to barrel 1, it should only partly dissociate during the wash with barrel 2. The fraction remaining during the exposure to barrel 3 should then transiently augment the response to NMDA above the level activated by the contaminating glycine in barrel 3. Regardless of the glycine concentration in barrel 1, the fraction of previously bound glycine still remaining at any time after glycine removal should in all cases be the same if a measurement is made at a constant time following the wash with barrel 2. That fraction will depend on the dissociation rate of glycine in the absence of NMDA (see below) and on the delay from glycine removal to time of measurement. The magnitude of the augmentation of the NMDA response

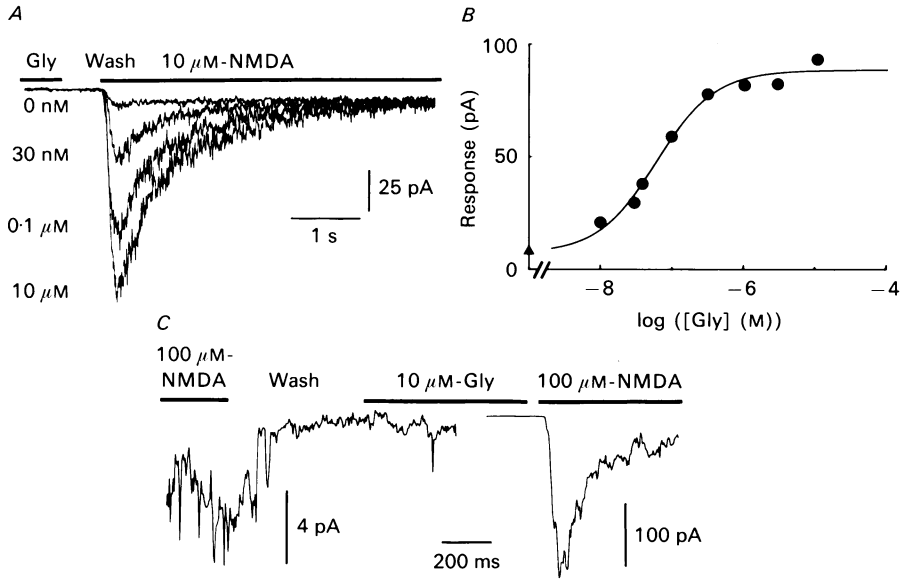

Fig. 6. Dissociation constant of glycine in the absence of NMDA. *A*, averaged whole-cell currents used to estimate how much glycine was bound before the application of NMDA. The cell was fast perfused with the indicated concentration of glycine (barrel 1) for at least 10 s, the solution perfusing the cell was changed to control solution (barrel 2), and after a 0·5 s wash the solution was changed to 10 μM-NMDA with no added glycine (barrel 3). Examples of responses to four different glycine concentrations are superimposed. Each trace is the average of four to eight recordings. Data were filtered at 100 Hz and sampled at 250 Hz. *B*, C–R curve for glycine in the absence of NMDA. Data are from the same cell as used for *A*, and were measured using the same protocol. On the abscissa is the concentration of glycine present in barrel 1. On the ordinate is response magnitude measured after the exposure to 10 μM-NMDA in barrel 3. Response magnitude was measured as the average current during a 50 ms period centred 0·5 s following the change to NMDA (barrel 3). The current baseline was measured as the average current during the 0·5 s wash with control solution (barrel 2). The data are fitted as described in Methods by eqn (1). The response magnitude in the absence of added glycine (R_0) was 7·2 pA (▲ on the *y*-axis); (●) other response magnitudes. The fit parameter values are: R_M, 89 pA; K_D, 61 mM; n_H, 1·07. The value of r^2 for the fit was 0·989. Similar measurements were performed in two other whole-cell experiments. Measurements at eight or nine different glycine concentrations were made in each cell. *C*, unaveraged data from the same cell as in *A* and *B*. On the left, the cell was first exposed to 100 μM-NMDA (barrel 1), then to control solution (barrel 2) for 0·5 s, and then to 10 μM-glycine (barrel 3). The absence of a response to 10 μM-glycine indicates that the NMDA from barrel 1 fully dissociated and was completely washed away during the 0·5 s wash. In order to gauge the sensitivity of this measurement to any NMDA that had not been washed away, the response to a jump from 10 μM-glycine (barrel 3) directly into 100 μM-NMDA (barrel 1; barrel 2 briefly washed the cell in transit) is shown on the right. Note the difference in current scales. Data were filtered at 100 Hz and sampled at 250 Hz.

during perfusion by barrel 3 can thus be used as an index of the glycine site occupancy during perfusion by barrel 1.

It was found that the response to the 10 μM-NMDA in barrel 3 was augmented in a glycine concentration-dependent manner by the previous exposure to glycine in barrel 1 (Fig. 6*A*). A C–R curve for the binding of glycine to functional NMDA

receptors in the absence of an NMDA agonist was constructed by plotting the response magnitude measured after exposure to 10 μM-NMDA (in barrel 3) as a function of the glycine concentration to which the cell was previously exposed (in barrel 1). The data were fitted as described earlier for C–R curves (Fig. 6*B*). From three experiments, the glycine apparent dissociation constant was 80 ± 10 nM and the Hill coefficient was $1{\cdot}22 \pm 0{\cdot}13$. The K_D measured in the absence of NMDA is significantly different from the K_D of 150 nM measured in the presence of 10 μM-NMDA ($P < 0{\cdot}005$, two-tailed Mann–Whitney test). The value of n_H measured in the absence of NMDA is not significantly different from the n_H of 1·11 measured from complete C–R curves in the presence of 10 μM-NMDA ($P > 0{\cdot}2$, two-tailed Mann–Whitney test). The value of n_H measured in the absence of NMDA is greater than 1 with marginal significance ($0{\cdot}02 < P < 0{\cdot}05$, Student's one-tailed t test). The mean value of r^2 for the three fits was 0·991.

The glycine K_D estimated in these experiments can be corrected for glycine contamination (Appendix 1) in the same manner as was the K_D estimated from glycine C–R curves measured in 10 μM-NMDA. The corrected value of K_D was found to be 70 ± 10 nM ($n = 3$).

The validity of these data depends on whether or not the removal of unbound glycine during the 0·5 s wash with barrel 2 was complete. If a fraction of glycine not bound to the NMDA receptor was washed out very slowly, then the barrel 3 response could have been due to augmentation of the response by that remaining glycine. Figure 3*A* argues that the change of the solution surrounding a cell is nearly complete in much less than 0·5 s, but the experiment was not very sensitive to the possibility that a small fraction of the surrounding drug washes out slowly. A different protocol was used to determine if the 0·5 s wash with the barrel 2 solution was sufficient to completely remove the barrel 1 solution from around the cell before exposure to the barrel 3 solution. The cell was first exposed to NMDA in barrel 1, then a 0·5 s wash was performed with barrel 2, and then the cell was exposed to glycine with barrel 3. Because the dissociation rate of NMDA is much faster than that of glycine, the wash period should allow for the complete removal of bound as well as unbound NMDA. However, if the wash with barrel 2 did not wash away all of the NMDA in barrel 1, then an NMDA response would be visible during exposure to the glycine in barrel 3. In order to reveal more sensitively an incomplete wash of the barrel 1 solution, a high NMDA concentration (100 μM) was used in barrel 1. In Fig. 6*C*, the above protocol can be seen to result in no response to the application of 10 μM-glycine with barrel 3, indicating that the barrel 1 solution was effectively removed by the wash with barrel 2.

The kinetics of the interaction of glycine with functional NMDA receptors in the absence of NMDA agonists were also investigated. The dissociation rate of glycine was measured with 1 μM-glycine in barrel 1, control solution in barrel 2, and 10 μM-NMDA in barrel 3. Following perfusion of the cell for at least 10 s with barrel 1, the cell was perfused with barrel 2 for a length of time that was varied, and then was perfused with barrel 3. The glycine bound to the NMDA receptor during perfusion with barrel 1 dissociated in the absence of NMDA agonists during perfusion with barrel 2. The relative amount of glycine that remained bound following the barrel 2 wash was measured as the current induced by perfusion of NMDA by barrel 3 (Fig.

7*A*). The time course of dissociation was measured by plotting the current magnitude measured after exposure to 10 μM-NMDA (in barrel 3) as a function of the barrel 2 wash time (Fig. 7*B*). The decay time constant was measured by fitting (as described in Methods) a single exponential to the data with response at time 0, steady state

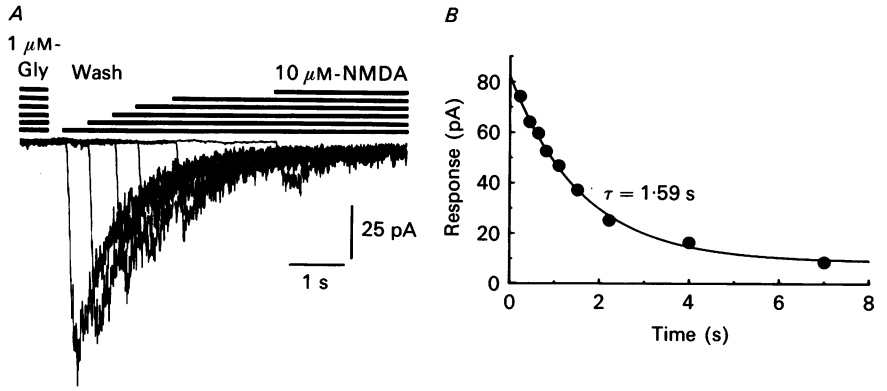

Fig. 7. Dissociation rate of glycine in the absence of NMDA. *A*, averaged whole-cell current used to estimate how much glycine was still bound after a wash of variable duration with solution containing no added glycine or NMDA. The cell was fast perfused with 1 μM-glycine (barrel 1) for at least 10 s, the solution perfusing the cell was changed to control solution (barrel 2), and after a wash of the duration indicated in the figure, the solution was changed to 10 μM-NMDA with no added glycine (barrel 3). Examples of responses after six different wash durations (0·2, 0·6, 1·1, 1·5, 2·2 and 4·0 s) are superimposed. Note that, following each jump into NMDA following a wash of longer than 0·2 s wash time, the peak current rises above the current traces from jumps following shorter wash times. The higher peak is probably in part due to desensitization of previous responses, but may also reflect a tendency for glycine to dissociate slightly more slowly in the absence of NMDA. Each trace is the average of three recordings. Data were filtered at 100 Hz and sampled at 250 Hz. *B*, data from the cell used for *A*. On the abscissa is the duration of the wash with control solution (barrel 2). On the ordinate is the response magnitude measured after the exposure to 10 μM-NMDA in barrel 3. Response magnitude was measured as the average current during a 50 ms period centred 0·5 s following the change to NMDA (barrel 3). The current baseline was measured as the average current during the last 0·5 s before the jump to 10 μM-NMDA. The data are fitted as described in Methods by a single exponential decay (see Results). The fit parameter values are: response at time 0, 83 pA; time constant of decay, 1·59 s; steady state response, 8·6 pA. The value of r^2 for the fit is 0·997. Similar fits were performed in two other whole-cell experiments. These data can be used to make a gross estimate of the expected magnitude of the response to a jump from 1 μM-glycine to 1 μM-glycine plus 10 μM-NMDA, assuming that glycine can bind to the same number of NMDA receptors in the absence and presence of NMDA. If the response at $t = 0$ is extrapolated back 0·5 s (necessary because the response was measured at 0·5 s after the jump to NMDA, and glycine continued to dissociate from its receptor during this 0·5 s), the predicted response magnitude is 110 pA. This correlates well with the measured peak response of 120 pA observed following a concentration jump from 1 μM-glycine to 1 μM-glycine plus 10 μM-NMDA. The similarity of these values suggests that glycine was able to bind to all functional NMDA receptors in the absence of NMDA.

response, and time constant as free parameters. Because the decay took place in the absence of NMDA or added glycine, the inverse of the time constant should approximate the dissociation rate constant in 0 NMDA. From three experiments, the glycine dissociation rate constant in the absence of NMDA was $0{\cdot}70 \pm 0{\cdot}22$ s^{-1}. The mean value of r^2 for the three fits was 0·987. The dissociation rate measured in the absence of NMDA is not significantly different from the dissociation rate measured from jumps into 0 glycine measured in the presence of 10 μM-NMDA ($P > 0{\cdot}1$, two-tailed Mann–Whitney test). In two additional experiments, this protocol was repeated with 100 nM instead of 1 μM-glycine in barrel 1. The mean value of the dissociation rate constant (0·70 s^{-1}) was consistent with the rate constants measured with 1 μM-glycine.

DISCUSSION

Glycine affinity and its possible modulation by NMDA

We have measured the apparent dissociation constant (K_D) of glycine using three different approaches. It was deduced from concentration–response curves in two series of experiments, one performed in the presence of 10 μM-NMDA, and the other designed to evaluate the K_D in the absence of NMDA. The first group of experiments gave a value for the K_D of 150 nM, while the second gave a value of 80 nM. The K_D was also independently estimated as the ratio of the rate of dissociation (k_-) to the rate of association (k_+). This ratio (k_-/k_+) was found to be 90 nM. All three values appear to be in reasonable agreement, considering the variability often encountered in estimates of apparent dissociation constants.

All three values are likely to be overestimated due to the presence of contaminating glycine. The values estimated from C–R curves can be corrected for the glycine contamination if, as suggested by Kleckner & Dingledine (1988), glycine binding is necessary for the NMDA response. This idea was supported by the observation that when extensive efforts were made to minimize glycine contamination, the response to 10 μM-NMDA in the absence of added glycine became very small (in some cases less than 2% of the response to 10 μM-NMDA plus a saturating concentration of glycine). We present here no direct evidence that the relative large NMDA responses sometimes observed in the absence of added glycine were due exclusively to glycine contamination. However, the complete block of the NMDA response by some inhibitory drugs that bind at the glycine site (e.g., Kemp, Foster, Leeson, Priestley, Tridgett, Iversen & Woodruff, 1988; Foster & Kemp, 1989), and the kinetics of this block (Benveniste *et al.* 1990*b*; Henderson, Johnson & Ascher, 1990), suggest that all of the NMDA responses in the absence of added glycine that we observed depend almost entirely on contaminating glycine. This may not be a property of NMDA responses in all cell types (Sekiguchi, Okamoto & Sakai, 1990).

We therefore corrected the value of the glycine K_D for the error due to contaminating glycine as described in Appendix 1. The corrected value of the K_D measured in the absence of glycine was 70 nM, and the corrected K_D measured in 10 μM-NMDA was 130 nM.

K_D values in the range of 100 nM are at the low end of the numerous published values (see Thomson, 1990) which are mostly in the 100 to 700 nM range. However, it is worth noting that the earliest binding data suggested K_D's close to 100 nM

(DeFeudis *et al.* 1977; Kishimoto *et al.* 1981; Bristow *et al.* 1986) and that some recent electrophysiological studies also report values in this range (see, e.g., Huettner, 1989).

One possible explanation for the variability of K_D estimates is variation in the amount of contaminating glycine, for which corrections have rarely been attempted (see Vyklický *et al.* 1990). Another possibility is that glycine affinity is modulated by the binding of NMDA. The data on this point are in conflict; some binding experiments suggest a positive co-operative interaction between the binding of glycine and the binding of NMDA (Reynolds *et al.* 1987; Fadda, Danysz, Wroblewski & Costa, 1988; Monaghan, Olverman, Nguyen, Watkins & Cotman, 1988; Kessler *et al.* 1989; Hood, Compton & Monahan, 1990; but see Bonhaus *et al.* 1989), while some physiological experiments suggest either that NMDA binding decreases the affinity of glycine (Benveniste *et al.* 1990*a*) or that the effects of NMDA and glycine exhibit neither positive nor negative co-operativity (Lerma, Kushner, Zukin & Bennett, 1989; McBain, Kleckner, Wyrick & Dingledine, 1989).

The difference between the K_D's observed in 10 μM and 0 NMDA is statistically significant but small. We hesitate to draw any firm conclusions from this small change, considering the difference in measurement techniques used. It is nevertheless consistent with the suggestion of Benveniste *et al.* (1990*a*) that NMDA binding decreases glycine affinity. In the experiments of Benveniste *et al.* (1990*a*) the negative co-operativity between NMDA binding and glycine binding was associated with glycine-dependent desensitization, a process that we in general observed only when using relatively old neurons (see Sather *et al.* 1990). It is therefore possible that the small difference we observed between glycine affinity in 0 and 10 μM-NMDA would have been amplified if we had used larger neurons and shorter periods of intracellular perfusion, conditions that appear to favour the expression glycine-sensitive desensitization. It should be noted that 10 μM is below the K_D for NMDA (see, e.g., Patneau & Mayer, 1990). If NMDA binding does change the glycine K_D, then we would have measured, in 10 μM-NMDA, a glycine K_D between the dissociation constant with the NMDA site unoccupied and the dissociation constant with the site occupied. It would have been instructive to have made a comparison of the above data with measurements of the glycine K_D at saturating concentrations of NMDA. However, we felt that the complications introduced by desensitization made interpretation of such experiments too tentative to be useful.

The possible effect of NMDA on glycine affinity highlights an advantage of the measurements made in the absence of NMDA; the measured K_D should be equal to the glycine dissociation constant with the NMDA site unoccupied, regardless of any effects that NMDA binding may have on the glycine dissociation constant (see Appendix 2). An additional advantage is that in the absence of NMDA, the receptors should be minimally desensitized, so the measured K_D should have minimal interference from any affinity changes induced by desensitization.

The association and dissociation rates of glycine

Measurement of the time constants of current relaxations following glycine concentration jumps allowed evaluation of the rate constants of association (k_+) and dissociation (k_-) of glycine. The value found for k_+, $1{\cdot}2 \times 10^7$ M^{-1} s^{-1}, is in the same

range as the k_+ for the binding of other small ligands to receptor molecules, such as the binding of acetylcholine (ACh) to the nicotinic ACh receptor (10^7–10^8 M^{-1} s^{-1}; Boyd & Cohen, 1980; Sine & Steinbach, 1987; Colquhoun & Ogden, 1988). It agrees very well with the value estimated by Benveniste *et al.* (1990*a*) of $1{\cdot}1 \times 10^7$ M^{-1} s^{-1} in experiments similar to ours but performed at an NMDA concentration of 100 μM.

The dissociation rate constant for glycine, k_-, was evaluated with three separate approaches: (1) in the presence of 10 μM-NMDA, a line fitted to a plot of $1/\tau_{on}$ *vs.* [glycine] was extrapolated to the y-intercept and gave $k_- = 0{\cdot}8$ s^{-1}; (2) the mean value of $1/\tau_{off}$ in the presence of 10 μM-NMDA gave $k_- = 1{\cdot}0$ s^{-1}; and (3) the mean value of $1/\tau_{off}$ in the absence of NMDA (Fig. 7) gave $k_- = 0{\cdot}7$ s^{-1}. The value of $1/\tau_{off}$ that we measured at 10 μM-NMDA ($1{\cdot}0$ s^{-1}) is higher than that measured in the absence of NMDA ($0{\cdot}7$ s^{-1}). Although the difference is not significant, it is in the direction expected if NMDA binding decreases the affinity of glycine in part by increasing the dissociation rate. In an attempt to better evaluate this hypothesis, we performed a few experiments in higher NMDA concentrations (50 to 500 μM). In these experiments the relaxations following a jump to 0 added glycine were sometimes multiexponential, but their main component had a slow time constant (around 1 s). This observation suggests that the glycine dissociation constant is not greatly increased by NMDA binding, unless there is another process such as desensitization that has an offsetting effect.

The value of k_- for glycine has also been measured by Benveniste *et al.* (1990*a*), but in the presence of 100 rather than 10 or 0 μM-NMDA. These authors found for the extrapolated y-intercept of $1/\tau_{on}$ *vs.* [glycine] a value of $1{\cdot}1$ s^{-1}, in good agreement with our measurements, but found a much larger value of $3{\cdot}1$ s^{-1} for the mean value of $1/\tau_{off}$. These measurements present two discrepancies: first, between their and our value of $1/\tau_{off}$, and second, between their two estimates of k_-. Our experiments at higher NMDA concentrations suggest that the first discrepancy is not due to the difference in the NMDA concentration used. An alternative possibility is that the change from glycine-dependent desensitization, as usually observed in their experiments (Vyklický *et al.* 1990), to glycine-independent desensitization, as usually observed in ours (see Sather *et al.* 1990) reflects a change in cellular properties that extends to the kinetics of glycine binding. Another difference in experimental conditions that could influence glycine dissociation rate is extracellular Ca^{2+} concentration; Benveniste *et al.* (1990*a*) used $0{\cdot}2$ mM-Ca^{2+} while we used $1{\cdot}0$ mM-Ca^{2+}. Increasing extracellular Ca^{2+} concentration has been reported to decrease the apparent dissociation constant of glycine (Gu & Huang, 1991); this could be due to, at least in part, a decrease in the dissociation rate. Benveniste *et al.* (1990*a*) suggest that the second discrepancy, between their two estimates of k_-, can be explained by the presence of two glycine binding sites, a hypothesis not required by our data.

One or two glycine bindings sites?

The hypothesis that each NMDA receptor–channel complex bears two glycine binding sites was first made on the basis of binding data indicating that there are twice as many binding sites for glycine as for TCP, a ligand that is believed to bind to the NMDA channel (Thedinga, Benedict & Fagg, 1989; Yeh, Bonhaus, Nadler & McNamara, 1989; Yeh, Bonhaus & McNamara, 1990). More recently, Benveniste

et al. (1990*a*) and Benveniste & Mayer (1991) have found that a model using two binding sites was superior to a model with a single site in fitting the current relaxations observed after a glycine concentration jump. In contrast, a model with a single functional glycine binding site for each receptor molecule appears consistent with the following aspects of our data: (1) the Hill coefficient measured at the foot of the glycine C–R curve was found to be close to 1 under conditions in which we believe that we have excluded the possibility of an artifact due to glycine contamination; (2) the plot of $1/\tau_{on}$ *versus* glycine concentration was linear; (3) the value of k_- estimated independently from measurements of τ_{on} and measurements of τ_{off} were in agreement; and (4) the ratio k_-/k_+ of rate constants calculated assuming no co-operativity was similar to the K_D measured from C–R curves.

These data are not compatible with a model in which the opening of the channel requires the occupation of two glycine binding sites, whether or not there is positive binding co-operativity between the two sites. The data are not inconsistent, however, with all models involving multiple glycine binding sites. For example, a two site model in which the occupancy of either site is sufficient to permit channel activation cannot be excluded. Such a model would allow reconciliation of our data and the binding data. However, it would not account for the functional co-operativity suggested by Benveniste *et al.* (1990*a*) and Benveniste & Mayer (1991).

The question of how many functional glycine sites there are may be resolved in one of three ways. First, it may be that activation of the NMDA receptor can require the binding of either one or two glycine molecules, depending on experimental conditions. It is possible, for example, that the disappearance of glycine sensitive desensitization is associated with the loss of a second functional glycine binding site. Second, glycine binding at more than one site may be necessary for channel activation, in which case evidence for co-operativity has somehow been masked in our experiments. One possibility is that movement into or out of the glycine-insensitive desensitized state altered the relaxations following glycine concentration jumps in a manner that artifactually hid evidence for co-operativity. Because plausible kinetic models tend to contain many adjustable parameters, it is often not difficult to fit a variety of different models to a set of kinetic data. However, it does appear difficult to reconcile with a two-site model, our steady state data showing no evidence for co-operativity at the foot of the C–R curve. We therefore prefer the third possibility, that glycine binding at a single site is sufficient for channel activation, and the kinetic data of Benveniste *et al.* (1990*a*) and of Benveniste & Mayer (1991) could be well fitted by a modified model with a single glycine binding site. For example, the inclusion of an additional step in the transition from the closed to the open state, as suggested by Lester, Clements, Westbrook & Jahr (1990), might remove the need for a second glycine binding site in the model.

The results presented in this and related studies allow some firm conclusions. Under the conditions of our experiments, the interaction of glycine with the NMDA receptor is not subject to powerful regulation by NMDA binding. The most extreme case in which glycine binding cannot take place in the absence of NMDA can be rejected. Furthermore, while glycine binding may influence NMDA affinity, the dominant mechanism by which glycine binding regulates NMDA response magnitude is not through an indirect effect on NMDA binding or desensitization. The simplest plausible idea appears to be that the primary allosteric effect of glycine binding is on

channel gating, analogous to the action of NMDA on gating of the NMDA channel or of ACh on gating of the nicotinic ACh channel.

APPENDIX 1

Because of the presence of an unknown but significant concentration of glycine contaminating our solutions, our glycine C–R data represented the response as a function of added rather than true (added plus contaminating) glycine concentration. The procedure used to derive information from C–R data was to find the best fit of eqn (1) (the Hill equation modified to fit data with a response at 0 added agonist concentration) to these data. The question to be addressed in this appendix is: if the Hill equation describes the true glycine C–R curve, can the parameters derived from fitting eqn (1) to our C–R data be related to the true parameters that describe the interaction of glycine with the NMDA receptor? The premise of this question implies that there is no response to NMDA in the complete absence of glycine. If this is the case, and the response measured in the absence of added glycine is due to a background glycine contamination, then the Hill equation can be written:

$$R_G = \frac{R_M([G]_B+[G])^{n_H}}{([G]_B+[G])^{n_H}+(K_{DT})^{n_H}}, \tag{A1}$$

where $[G]_B$ is the background (contaminating) glycine concentration, K_{DT} is the true apparent dissociation constant (the dissociation constant that would be measured if actual rather than added glycine concentrations were used in the fitting of C–R curves), and the meaning of the other symbols is the same as for eqn (1).

This equation cannot be manipulated into the form of eqn (1). We could have derived the desired information by fitting eqn (A1) to the data, leaving R_M, $[G]_B$, K_{DT}, and n_H as free parameters. However, after noting that the C–R curves exhibit relatively little co-operativity, we decided to take advantage of the fact that in the special case that $n_H = 1$, eqn (A1) can be manipulated into the form of eqn (1) without requiring the addition of another free parameter. If $n_H = 1$, then eqn (A1) can be rewritten:

$$R_G = \frac{R_M[G]_B}{[G]_B+[G]+K_{DT}}+\frac{R_M[G]}{[G]_B+[G]+K_{DT}}. \tag{A2}$$

The first term of the right-hand side of eqn (A2) can be broken into a part dependent on, and another independent of, [G]:

$$\frac{R_M[G]_B}{([G]_B+[G]+K_{DT})}\frac{([G]_B+K_{DT})}{([G]_B+K_{DT})} = \frac{R_M[G]_B([G]_B+[G]+K_{DT})-R_M[G]_B[G]}{([G]_B+[G]+K_{DT})([G]_B+K_{DT})}$$

$$= \frac{R_M[G]_B}{[G]_B+K_{DT}}\left(1-\frac{[G]}{[G]_B+[G]+K_{DT}}\right). \tag{A3}$$

Substituting eqn (A3) back into eqn (A2) and rearranging gives:

$$R_G = \frac{R_M[G]_B}{[G]_B+K_{DT}}+\left(R_M-\frac{R_M[G]_B}{[G]_B+K_{DT}}\right)\left(\frac{[G]}{([G]_B+[G]+K_{DT})}\right). \tag{A4}$$

Recognizing that $(R_M[G]_B)/([G]_B+K_{DT})$ must equal R_0 (the response in the absence of added glycine; see eqn (1)), and defining $K_D = [G]_B+K_{DT}$, eqn (A4) can be

rewritten as eqn (1) with $n_H = 1$. The dissociation constant measured by fitting eqn (1) to data is larger than K_{DT} by an amount equal to $[G]_B$. This information can be used to estimate the background glycine concentration from the results of fitting eqn (1) to the data:

$$R_0 = \frac{R_M[G]_B}{[G]_B + K_{DT}} = \frac{R_M[G]_B}{K_D}.$$

$$[G]_B = \frac{R_0 K_D}{R_M}.$$

APPENDIX 2

The question to be addressed in this appendix is: how do the rate constants that characterize glycine binding relate to the time constant of macroscopic current relaxations following glycine concentrations jumps? In order to derive a simple formula for the relaxation time constant, the following assumptions will be made: (1) there is a single NMDA binding site (general consideration of two NMDA binding sites will be made at the end of the appendix); (2) the time constant characteristic of NMDA binding is much faster than that of glycine binding (see Results), so that any states separated only by an NMDA binding step can be considered in equilibrium during relaxations and only the dissociation constant (not rate constants) for NMDA binding needs to be used; (4) the time constant characteristic of channel transitions is much faster than that of glycine binding (see Results), so that similarly only the fraction of time that the fully liganded channel spends open needs to be used. The reaction scheme can then be written:

$$\begin{array}{ccccc} N+R+G & \overset{K_{N1}}{\leftrightarrow} & NR+G & & \\ k_{+1}\downarrow\uparrow k_{-1} & & k_{-2}\uparrow\downarrow k_{+2} & & \\ N+RG & \underset{K_{N2}}{\leftrightarrow} & NRG & \underset{K_o}{\leftrightarrow} & NRG^*, \end{array} \tag{A5}$$

where N is a molecule of NMDA, R is the NMDA receptor–channel complex, G is a molecule of glycine, NR is the complex with only NMDA bound, RG is the complex with only glycine bound, NRG is the complex with both NMDA and glycine bound, and NRG* is the fully liganded complex with the channel open (this is the only state with an open channel). K_{N1} and K_{N2} are dissociation constants, K_o is equal to [NRG]/[NRG*], and k_{+1}, k_{-1}, k_{+2}, and k_{-2}, are rate constants.

If R can be considered in equilibrium with NR during relaxations, then R and NR can be treated as a single state (combined state 1). Likewise, RG, NRG, and NRG* can be considered a single state (combined state 2). If k_{+1}' and k_{+2}' are the rate constants for the left-hand and the right-hand paths (scheme A5), respectively, from combined states 1 to 2, then:

$$k_{+1}' = \frac{[R]k_{+1}}{[R]+[NR]} = \frac{K_{N1}k_{+1}}{K_{N1}+[N]},$$

$$k_{+2}' = \frac{[NR]k_{+2}}{[R]+[NR]} = \frac{[N]k_{+2}}{K_{N1}+[N]}.$$

If k_{-1}' and k_{-2}' are the rate constants for the left-hand and right-hand paths (scheme (A5)), respectively, from combined states 2 to 1, then:

$$k_{-1}' = \frac{[\mathrm{RG}]k_{-1}}{[\mathrm{RG}]+[\mathrm{NRG}]+[\mathrm{NRG}^*]} = \frac{K_{\mathrm{N2}}k_{-1}}{K_{\mathrm{N2}}+[\mathrm{N}]+([\mathrm{N}]/K_0)},$$

$$k_{-2}' = \frac{[\mathrm{NRG}]k_{-2}}{[\mathrm{RG}]+[\mathrm{NRG}]+[\mathrm{NRG}^*]} = \frac{[\mathrm{N}]k_{-2}}{K_{\mathrm{N2}}+[\mathrm{N}]+([\mathrm{N}]/K_0)}.$$

When there is more than one path interconnecting two states, the reciprocal of the relaxation time constant is simply the sum of the rate constant terms (Bernasconi, 1976). Because the same relaxation time constant(s) must apply to all states of a reaction scheme, the time constant for relaxations between combined states 1 and 2 must also apply to relaxations of NRG*. Thus, since current is proportional to [NRG*], the reciprocal relaxation time constant of measured current of this system is:

$$1/\tau = (k_{+1}'+k_{+2}')[\mathrm{G}]+k_{-1}'+k_{-2}' = \frac{(K_{\mathrm{N1}}k_{+1}+[\mathrm{N}]k_{+2})[\mathrm{G}]}{(K_{\mathrm{N1}}+[\mathrm{N}])}+\frac{K_{\mathrm{N2}}k_{-1}+[\mathrm{N}]k_{-2}}{(K_{\mathrm{N2}}+[\mathrm{N}]+([\mathrm{N}]/K_0))}.$$

The relative contribution of the two glycine binding paths to the relaxation time constant depends on NMDA concentration. At low NMDA concentrations, the left-hand path of scheme (A5) will dominate, while at high NMDA concentrations the right-hand path will dominate. Note that, in the absence of NMDA, $1/\tau = k_{+1}[\mathrm{G}]+k_{-1}$. Even at intermediate NMDA concentrations, a single exponential is predicted. In the special case in which glycine binding is unaffected by NMDA binding ($k_{+1} = k_{+2}$ and $k_{-1} = k_{-2}$), and the fully liganded receptor–channel complex spends most of its time in the closed state ($K_0 \gg 1$, as suggested by Huettner & Bean, 1988, but see Jahr, 1992), then at any NMDA concentration $1/\tau = k_{+1}[\mathrm{G}]+k_{-1}$.

If there are two NMDA binding sites (see Patneau & Mayer, 1990; Benveniste & Mayer, 1991; Clements & Westbrook, 1991), then the same approach can be applied to a model that can be written:

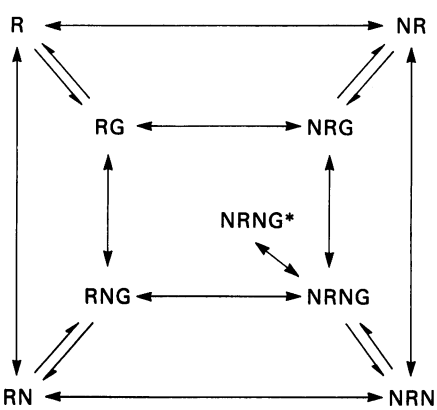

All transitions around the outer square, all transitions around the inner square, and the transition to the open channel would be fast. Only the transitions between the outer and the inner square (all transitions involving glycine binding) would be

rate limiting. Single exponential relaxations would still be predicted to follow glycine concentration jumps. If the binding of NMDA did not affect glycine binding, and the fully liganded channel spent the great majority of its time closed, then the reciprocal of the relaxation time constant could still be calculated as $k_{+1}[G]+k_{-1}$.

It should be remembered that NMDA binding and channel transition steps do not take place instantaneously, as would have to be the case for these equations to apply exactly. These additional steps should make the current relaxations sigmoid. Analysis of the initial sigmoid portion of the relaxation would require more rapid solution changes and more precise knowledge of the moment of solution change than was possible in the whole-cell experiments reported here (but see Clements & Westbrook, 1991).

We thank Boris Barbour for comments on the manuscript and Danielle Lévy for preparation of the cultures. This work was supported by the CNRS (URA 295), the Université Pierre et Marie Curie, INSERM (CRE 89 2001), the Human Frontiers Science Program, the Fondation pour la Recherche Médicale, the Ministère de la Recherche (89C 0702) and the National Institute of Mental Health (R29 MH45817). J.W.J. was supported in part by a National Research Service Award (F32 MH09313).

REFERENCES

ASCHER, P., BREGESTOVSKI, P. & NOWAK, L. (1988). *N*-methyl-D-aspartate-activated channels of mouse central neurones in magnesium-free solutions. *Journal of Physiology* **399**, 207–226.

ASCHER, P. & JOHNSON, J. W. (1989). The NMDA receptor, its channel, and its modulation by glycine. In *The NMDA Receptor*, ed. WATKINS, J. C. & COLLINGRIDGE, G. L., pp. 109–121. Oxford University Press, Oxford.

BENVENISTE, M., CLEMENTS, J., VYKLICKÝ L. JR & MAYER, M. L. (1990*a*). A kinetic analysis of the modulation of *N*-methyl-D-aspartic acid receptors by glycine in mouse cultured hippocampal neurones. *Journal of Physiology* **428**, 333–357.

BENVENISTE, M. & MAYER, M. L. (1991). Kinetic analysis of antagonist action at *N*-methyl-D-aspartic acid receptors. *Biophysical Journal* **59**, 560–573.

BENVENISTE, M., MIENVILLE, J.-M., SERNAGOR, E. & MAYER, M. L. (1990*b*). Concentration jump experiments with NMDA antagonists in mouse cultured hippocampal neurons. *Journal of Neurophysiology* **63**, 1373–1384.

BERNASCONI, C. F. (1976). *Relaxation Kinetics*. Academic Press, New York.

BONHAUS, D. W., YEH, G. C., SKARYAK, L. & MCNAMARA, J. O. (1989). Glycine regulation of the *N*-methyl-D-aspartate receptor-gated ion channel in hippocampal membranes. *Molecular Pharmacology* **36**, 273–279.

BOYD, N. D. & COHEN, J. B. (1980). Kinetics of binding of [^{3}H] acetylcholine and [^{3}H]carbamoylcholine to *Torpedo* postsynaptic membranes: slow conformational transitions of the cholinergic receptor. *Biochemistry* **19**, 5344–5353.

BRISTOW, D. R., BOWERY, N. G. & WOODRUFF, G. N. (1986). Light microscopic autoradiographic localisation of [^{3}H]glycine and [^{3}H]strychnine binding sites in rat brain. *European Journal of Pharmacology* **126**, 303–308.

CACECI, M. S. & CACHERIS, W. P. (1984). Fitting curves to data, the simplex algorithm is the answer. *Byte* **9**, 340–362.

CLARK, G. D., CLIFFORD, D. B. & ZORUMSKI, C. F. (1990). The effect of agonist concentration, membrane voltage and calcium on *N*-methyl-D-aspartate receptor desensitization. *Neuroscience* **39**, 787–797.

CLEMENTS, J. D. & WESTBROOK, G. L. (1991). Activation kinetics used to determine number of binding sites on the Ca^{2+} channel. *Biophysical Journal* **59**, 353a.

COLLINGRIDGE, G. L. & LESTER, R. A. J. (1989). Excitatory amino acid receptors in the vertebrate central nervous system. *Pharmacological Reviews* **40**, 143–210.

COLQUHOUN, D. & OGDEN, D. C. (1988). Activation of ion channels in the frog end-plate by high concentrations of acetylcholine. *Journal of Physiology* **395**, 131–159.

DEFEUDIS, F. V., FANDO, J. & ORENSANZ MUÑOZ, L. M. (1977). 'High-affinity' binding sites for glycine in synaptosomal-mitochondrial fractions of rat CNS regions. *Experientia* **33**, 1068–1070.

FADDA, E., DANYSZ, W., WROBLEWSKI, J. T. & COSTA, E. (1988). Glycine and D-serine increase the affinity of N-methyl-D-aspartate sensitive glutamate binding sites in rat brain synaptic membranes. *Neuropharmacology* **27**, 1183–1185.

FONG, T. M., DAVIDSON, N. & LESTER, H. A. (1988). Properties of two classes of rat brain acidic amino acid receptors induced by distinct mRNA populations in *Xenopus* oocytes. *Synapse* **2**, 657–665.

FOSTER, A. C. & KEMP, J. A. (1989). HA-966 antagonizes *N*-methyl-D-aspartate receptors through a selective interaction with the glycine modulatory site. *Journal of Neuroscience* **9**, 2191–2196.

GU, Y. & HUANG, L.-Y. M. (1991). Ca ions change the affinity of glycine to NMDA receptor complex. *Society for Neuroscience Abstracts* **17**, 1167.

HAMILL, O. P., MARTY, A., NEHER, E., SAKMANN, B. & SIGWORTH, F. J. (1981). Improved patch-clamp techniques for high-resolution current recording from cells and cell-free membrane patches. *Pflügers Archiv* **391**, 85–100.

HENDERSON, G., JOHNSON, J. W. & ASCHER, P. (1990). Competitive antagonists and partial agonists at the glycine modulatory site of the mouse *N*-methyl-D-aspartate receptor. *Journal of Physiology* **430**, 189–212.

HOOD, W. F., COMPTON, R. P. & MONAHAN, J. B. (1990). *N*-methyl-D-aspartate recognition site ligands modulate activity at the coupled glycine recognition site. *Journal of Neurochemistry* **54**, 1040–1046.

HOWE, J. R., COLQUHOUN, D. & CULL-CANDY, S. G. (1988). On the kinetics of large-conductance glutamate-receptor ion channels in rat cerebellar granule neurons. *Proceedings of the Royal Society* B **233**, 407–422.

HOWE, J. R., CULL-CANDY, S. G. & COLQUHOUN, D. (1991). Currents through single glutamate receptor channels in outside-out patches from rat cerebellar granule cells. *Journal of Physiology* **432**, 143–202.

HUETTNER, J. E. (1989). Indole-2-carboxylic acid: A competitive antagonist of potentiation by glycine at the NMDA receptor. *Science* **243**, 1611–1613.

HUETTNER, J. E. & BEAN, B. P. (1988). Block of *N*-methyl-D-aspartate-activated current by the anticonvulsant MK-801: selective binding to open channels. *Proceedings of the National Academy of Sciences of the USA* **85**, 1307–1311.

JAHR, C. E. (1992). High probability opening of NMDA receptor channels by L-glutamate. *Science* **255**, 470–472.

JAHR, C. E. & STEVENS, C. F. (1987). Glutamate activates multiple single channel conductances in hippocampal neurons. *Nature* **325**, 522–525.

JOHNSON, J. W. & ASCHER, P. (1987*a*). Glycine potentiates the NMDA response in cultured mouse brain neurons. *Nature* **325**, 529–531.

JOHNSON, J. W. & ASCHER, P. (1987*b*). Interaction of glycine with the N-methyl-D-aspartate receptor. *Society for Neuroscience Abstracts* **13**, 383.

KEMP, J. A., FOSTER, A. C., LEESON, P. D., PRIESTLEY, T., TRIDGETT, R., IVERSEN, L. L. & WOODRUFF, G. N. (1988). 7-chlorokynurenic acid is a selective antagonist at the glycine modulatory site of the *N*-methyl-D-aspartate receptor complex. *Proceedings of the National Academy of Sciences of the USA* **85**, 6547–6550.

KESSLER, M., TERRAMANI, T., LYNCH, G. & BAUDRY, M. (1989). A glycine site associated with *N*-methyl-D-aspartic acid receptors: Characterization and identification of a new class of antagonists. *Journal of Neurochemistry* **52**, 1319–1328.

KISHIMOTO, H., SIMON, J. R. & APRISON, M. H. (1981). Determination of the equilibrium dissociation constants and number of glycine binding sites in several areas of the rat central nervous system, using a sodium-independent system. *Journal of Neurochemistry* **37**, 1015–1024.

KLECKNER, N. W. & DINGLEDINE, R. (1988). Requirement for glycine in activation of NMDA-receptors expressed in *Xenopus* oocytes. *Science* **241**, 835–837.

KUSHNER, L., LEMA, J., ZUKIN, R. S. & BENNETT, M. V. L. (1988). Coexpression of *N*- methyl-D-aspartate and phencyclidine receptors in *Xenopus* oocytes injected with rat brain mRNA. *Proceedings of the National Academy of Sciences of the USA* **85**, 3250–3254.

LERMA, J., KUSHNER, L., ZUKIN, R. S. & BENNETT, M. V. L. (1989). *N*-methyl-D-aspartate activates different channels than do kainate and quisqualate. *Proceedings of the National Academy of Sciences of the USA* **86**, 2083–2087.

LESTER, R. A. J., CLEMENTS, J. D., WESTBROOK, G. L. & JAHR, C. E. (1990). Channel kinetics determine the time course of NMDA receptor-mediated synaptic currents. *Nature* **346**, 565–567.

MCBAIN, C. J., KLECKNER, N. W., WYRICK, S. & DINGLEDINE, R. (1989). Structural requirements for activation of the glycine coagonist site of *N*-methyl-D-aspartate receptors expressed in *Xenopus* oocytes. *Molecular Pharmacology* **36**, 556–565.

MAYER, M. L., MACDERMOTT, A. B., WESTBROOK, G. L., SMITH, S. J. & BARKER, J. L. (1987). Agonist- and voltage-gated calcium entry in cultured mouse spinal cord neurons under voltage clamp measured using arsenazo III. *Journal of Neuroscience* **7**, 3230–3244.

MAYER, M. L. & WESTBROOK, G. L. (1985). The action of *N*-methyl-D-aspartic acid on mouse spinal neurones in culture. *Journal of Physiology* **361**, 65–90.

MONAGHAN, D. T., OLVERMAN, H. J., NGUYEN, L., WATKINS, J. C. & COTMAN, C. W. (1988). Two classes of *N*-methyl-D-aspartate recognition sites: Differential distribution and differential regulation by glycine. *Proceedings of the National Academy of Sciences of the USA* **85**, 9836–9840.

NOWAK, L., BREGESTOVSKI, P., ASCHER, P., HERBET, A. & PROCHIANTZ, A. (1984). Magnesium gates glutamate-activated channels in mouse central neurones. *Nature* **307**, 462–465.

PATNEAU, D. K. & MAYER, M. L. (1990). Structure–activity relationships for amino acid transmitter candidates acting at *N*-methyl-D-aspartate and quisqualate receptors. *Journal of Neuroscience* **10**, 2385–2399.

REYNOLDS, I. J., MURPHY, S. N. & MILLER, R. J. (1987). ^{3}H-labeled MK-801 binding to the excitatory amino acid receptor complex from rat brain is enhanced by glycine. *Proceedings of the National Academy of Sciences of the USA* **84**, 7744–7748.

SATHER, W., DIEUDONNÉ, S., MACDONALD, J. F. & ASCHER, P. (1992). Activation and desensitization of *N*-methyl-D-aspartate receptors in nucleated outside-out patches from mouse neurones. *Journal of Physiology* **450**, 643–672.

SATHER, W., JOHNSON, J. W., HENDERSON, G. & ASCHER, P. (1990). Glycine-insensitive desensitization of NMDA responses in cultures mouse embryonic neurons. *Neuron* **4**, 725–731.

SEKIGUCHI, M., OKAMOTO, K. & SAKAI, Y. (1990). Glycine-insensitive NMDA-sensitive receptor expressed in *Xenopus* oocytes by guinea pig cerebellar mRNA. *Journal of Neuroscience* **10**, 2184–2155.

SHIRASAKI, T., NAKAGAWA, T., WAKAMORI, M., TATEISHI, N., FUKUDA, A., MURASE, K. & AKAIKE, N. (1990). Glycine-insensitive desensitization of *N*-methyl-D-aspartate receptors in acutely isolated mammalian central neurons. *Neuroscience Letters* **108**, 93–98.

SINE, S. M. & STEINBACH, J. H. (1987). Activation of acetylcholine receptors on clonal mammalian BC3H-1 cells by high concentrations of agonist. *Journal of Physiology* **385**, 325–359.

SNELL, L. D., MORTER, R. S. & JOHNSON, K. M. (1988). Structural requirements for activation of the glycine receptor that modulates the *N*-methyl-D-aspartate operated ion channel. *European Journal of Pharmacology* **156**, 105–110.

THEDINGA, K. H., BENEDICT, M. S. & FAGG, G. E. (1989). The *N*-methyl-D-aspartate (NMDA) receptor complex: A stoichiometric analysis of radioligand binding domains. *Neuroscience Letters* **104**, 217–222.

THOMSON, A. (1990). Glycine is a coagonist at the NMDA receptor/channel complex. *Progress in Neurobiology* **35**, 53–76.

VYKLICKÝ, L. JR, BENVENISTE, M. & MAYER, M. L. (1990). Modulation of *N*-methyl-D-aspartic acid receptor desensitization by glycine in mouse cultured hippocampal neurones. *Journal of Physiology* **428**, 313–331.

YEH, G.-C., BONHAUS, D. W. & MCNAMARA, J. O. (1990). Evidence that zinc inhibits *N*-methyl-D-aspartate receptor-gated ion channel activation by noncompetitive antagonism of glycine binding. *Molecular Pharmacology* **38**, 14–19.

YEH, G.-C., BONHAUS, D. W., NADLER, J. V. & MCNAMARA, J. O. (1989). *N*-methyl-D-aspartate receptor plasticity in kindling: quantitative and qualitative alterations in the *N*-methyl-D-aspartate receptor-channel complex. *Proceedings of the National Academy of Sciences of the USA* **86**, 8157–8160.